Supplementary materials

Inertial co-focusing of heterogeneous particles in hybrid microfluidic channels with constantly variable cross-sections

Tianwei Zhao,[a] Peng Zeng,[a] Yuanting Zhang,[b] Jinxia Li,[c] Hui Sun,[c] Imrich Gablech,[d] Honglong Chang,[b] Xichen Yuan,*[b] Pavel Neužil,*[b] and Jianguo Feng*[a]

[a]School of Microelectronics, Hefei University of Technology, Hefei, 230601, China

[b]Ministry of Education Key Laboratory of Micro and Nano Systems for Aerospace, School of Mechanical Engineering, Northwestern Polytechnical University, Xi'an, 710072, China

[c]Department of Medical Laboratory, Xi'an International Medical Centre Hospital, Xi'an 710100, China

[d]Department of Microelectronics, FEEC, Brno University of Technology, Technicka 10, CZ-616 00 Brno, Czech Republic

Corresponding authors:

Jianguo Feng: fengjg@hfut.edu.cn

Xichen Yuan: xichen.yuan@nwpu.edu.cn

Pavel Neužil: pavel.neuzil@nwpu.edu.cn

The design of HMC B, C, and D

HMC B (Fig. S1A): The outer wall of HMC B was a three-quarter circle arc with a curvature radius of 5,100 μm (R_1), and the inner wall was a three-quarter helix with radii of 4,500 μm (R_2) and 4,800 μm (R_4). This caused the main channel width of HMC B gradually decreasing from 600 μm (inlet, W_1) to 300 μm (outlet, W_2). Twenty semi-circular obstacles were distributed on the inner wall of HMC B with an identical angular distance between adjacent obstacles of $\alpha = 13°$. The radii of the obstacles (r_2) were determined by a three-quarter helix with radii of 4,800 μm (R_3) and 4,950 μm (R_5), and thus the height of obstacles gradually decreased from 300 μm (first obstacle near the inlet) to 150 μm (the last obstacle near the outlet). The obstacles were smoothly filtered by 300 μm (r_1) and 1,000 μm (r_3).

HMC C (Fig. S1B): Both outer and inner walls of HMC C were three-quarter circle arcs with curvature radii of 5,100 μm (R_1) and 4,900 μm (R_2=R_4), respectively. This induced an uniform main channel width of 200 μm (W_1=W_2) from inlet to outlet in HMC C. Twenty semi-circular obstacles were distributed on the inner wall with an identical angular distance adjacent obstacles of $\alpha = 13°$. The radii of the obstacles (r_2) were determined by a three-quarter helix with radii of 5,000 μm (R_3) and 5,050 μm (R_5), and thus the height of obstacles gradually increased from 100 μm (first obstacle near the inlet) to 150 μm (the last obstacle near the outlet). The obstacles were smoothly filtered by 300 μm (r_1) and 1,000 μm (r_3).

HMC D (Fig. S1C): Both outer and inner walls of HMC D were three-quarter circle arcs with curvature radius of 5,100 μm (R_1) and 4,900 μm (R_2=R_4), respectively. This induced an uniform main channel width of 200 μm (W_1=W_2) from inlet to outlet in HMC D. Twenty semi-circular obstacles with radii of 100 μm ($R_3 = R_5 = 5{,}000$ μm) were distributed on the inner wall with an identical angular distance between adjacent obstacles of $\alpha = 13°$. The obstacles were smoothly filtered by 300 μm (r_1) and 1,000 μm (r_3).

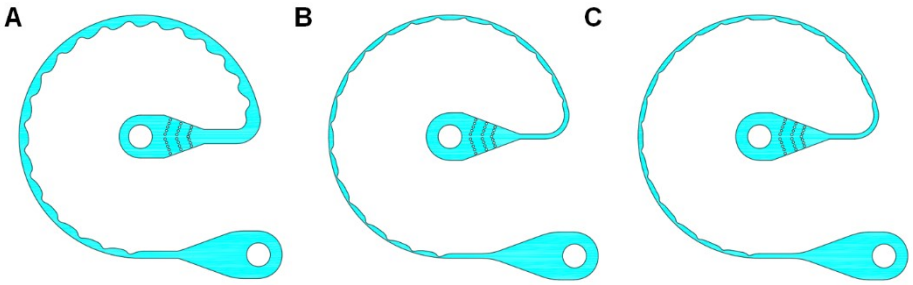

Fig. S1 The design of HMC B, C, and D.

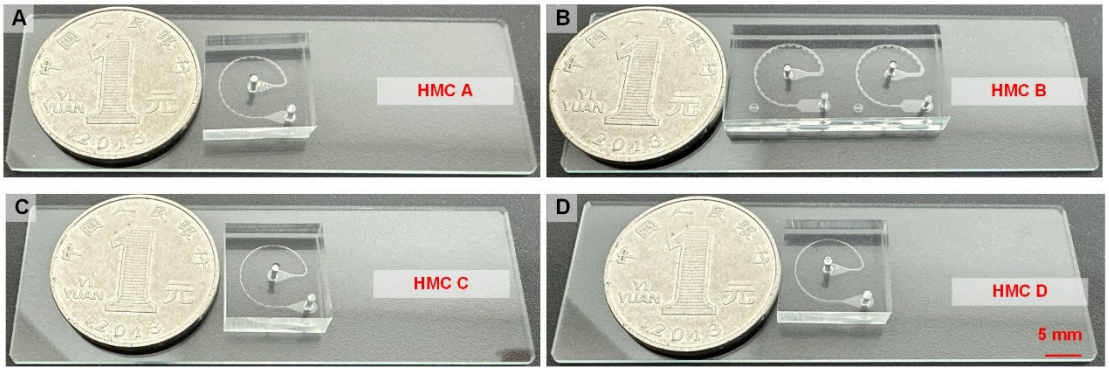

Fig. S2 The fabricated chips of HMC A, B, C, and D using standard soft lithography technique and PDMS molding processes. The coin of one Chinese RMB is used for comparison. The scale bar is 5 mm.

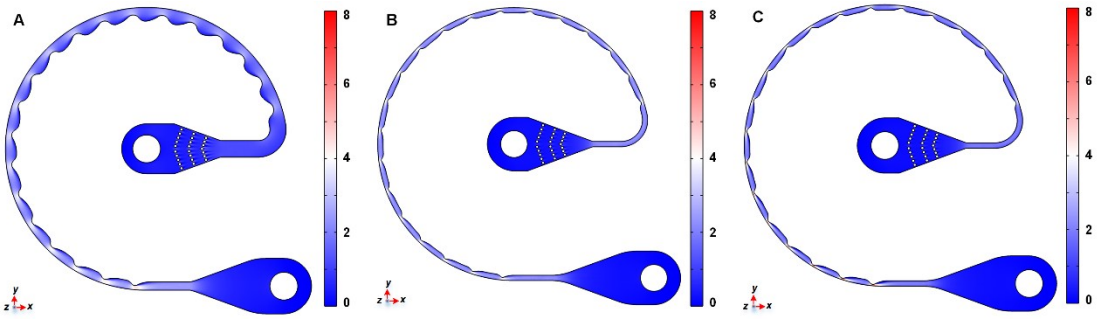

Fig. S3 The color contours indicating main flow velocity magnitude in HMC B, C, and D.

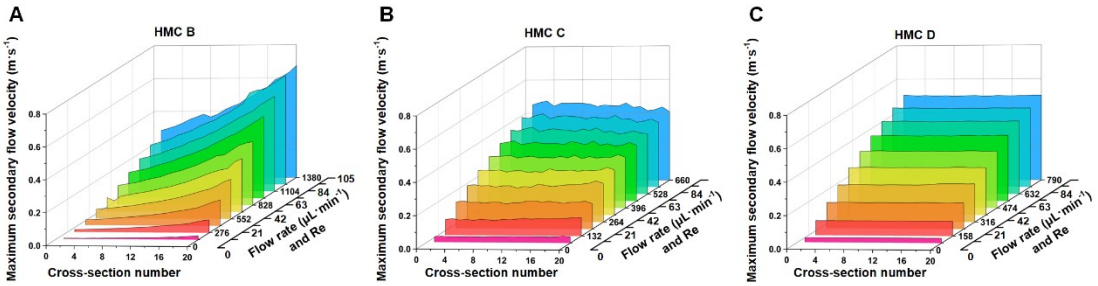

Fig. S4 The maximum secondary flow velocity as functions of cross-section number and flow rate (Re) in HMC B, C, and D. The flow rates vary from 138 to 1,380 μL·min^{-1} in HMC B, from 66 to 660 μL·min^{-1} in HMC C, and from 79 to 790 μL·min^{-1} in HMC D, resulting in identical Re ranging from 10.5 to 105.

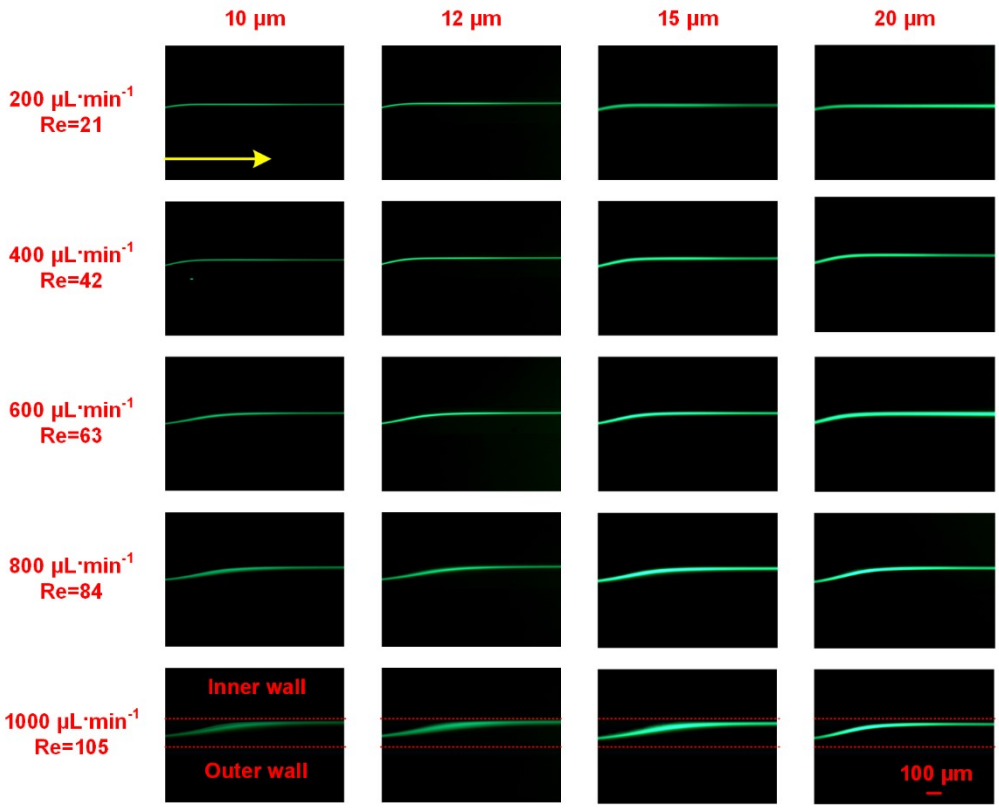

Fig. S5 The fluorescent streaks at the observation area in HMC A at different flow rates of 200 μL·min^{-1}, 400 μL·min^{-1}, 600 μL·min^{-1}, 800 μL·min^{-1}, and 1,000 μL·min^{-1}. The particle diameters are 10 μm, 12 μm, 15 μm, and 20 μm. The yellow arrow shows the fluid flow direction. The red dashed lines represent the channel walls. The scale bar is 100 μm. More images can be provided by reasonable requirements.

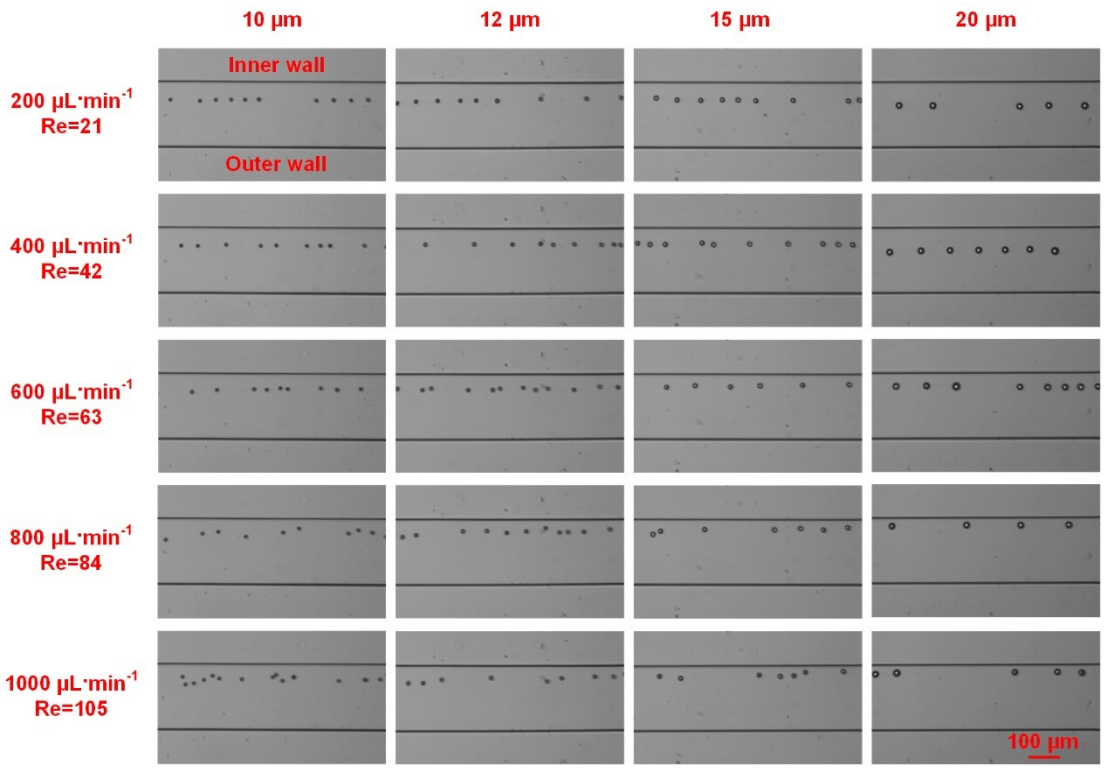

Fig. S6 The images of focused particles captured by a high-speed CCD camera at flow rates of 200 μL·min^{-1}, 400 μL·min^{-1}, 600 μL·min^{-1}, 800 μL·min^{-1}, and 1,000 μL·min^{-1}. The particle diameters are 10 μm, 12 μm, 15 μm, and 20 μm. The scale bar is 100 μm. More images can be provided by reasonable requirements.

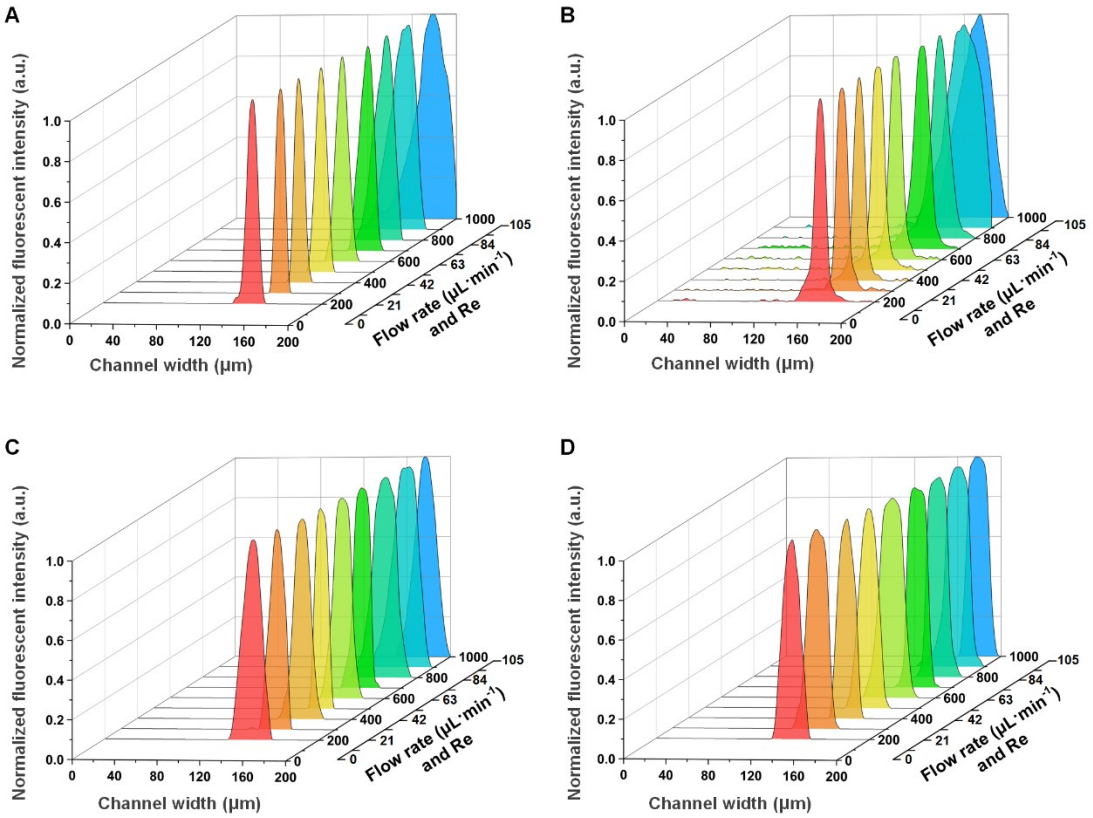

Fig. S7 The fluorescent intensity profiles of fluorescent streak images captured at the observation areas in HMC A with particle diameters of 10 μm (A), 12 μm (B), 15 μm (C), and 20 μm (D). The flow rates vary from 200 to 1,000 μL·min^{-1} (Re: 21 ~ 105).

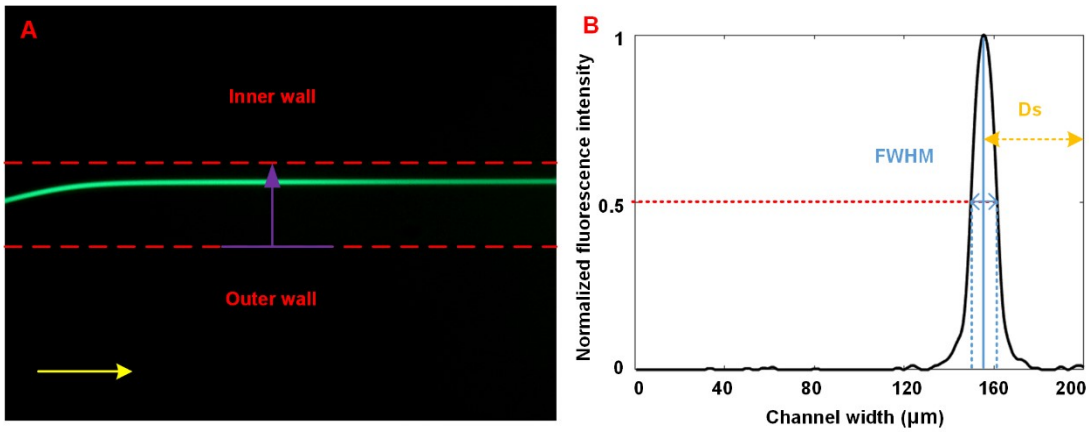

Fig. S8 (A) The fluorescent streak of particle focusing. The yellow arrow shows the fluid flow direction. The red dashed lines represent the channel walls. The purple arrow indicates the position and direction of image processing. (B) The illustration of full width at half maximum and *D*s (the distance between the fluorescent streak center and the inner wall) for the determination of focusing width and focusing position.

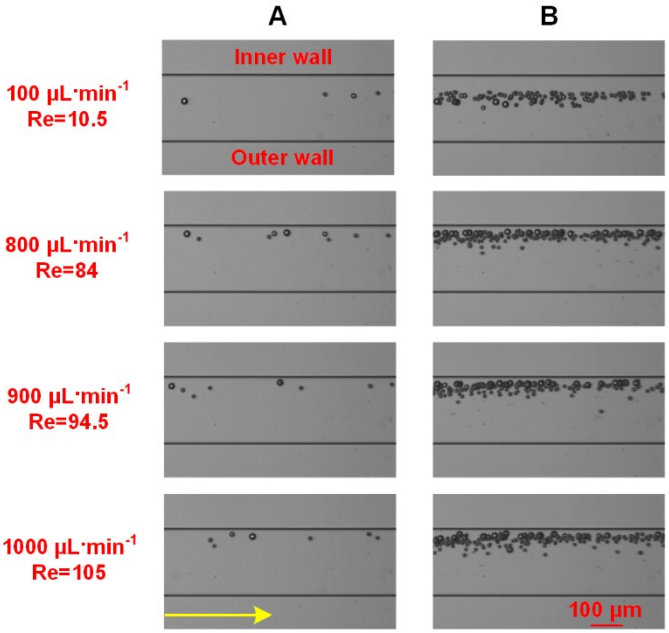

Fig. S9 (A) The images of focused multi-sized particles captured by a high-speed CCD camera at flow rates of 100 μL·min^{-1}, 800 μL·min^{-1}, 900 μL·min^{-1} and 1,000 μL·min^{-1} in HMC A. A particle mixture with a ratio of 1:1:1:1 of 10 μm, 12 μm, 15 μm, and 20 μm particles are prepared for the co-focusing experiments. The yellow arrow shows the fluid flow direction. (B) The composite images of focused multi-sized particles using 50 single images at flow rates of 100 μL·min^{-1}, 800 μL·min^{-1}, 900 μL·min^{-1} and 1,000 μL·min^{-1} in HMC A. The scale bar is 100 μm. More images can be provided by reasonable requirements.

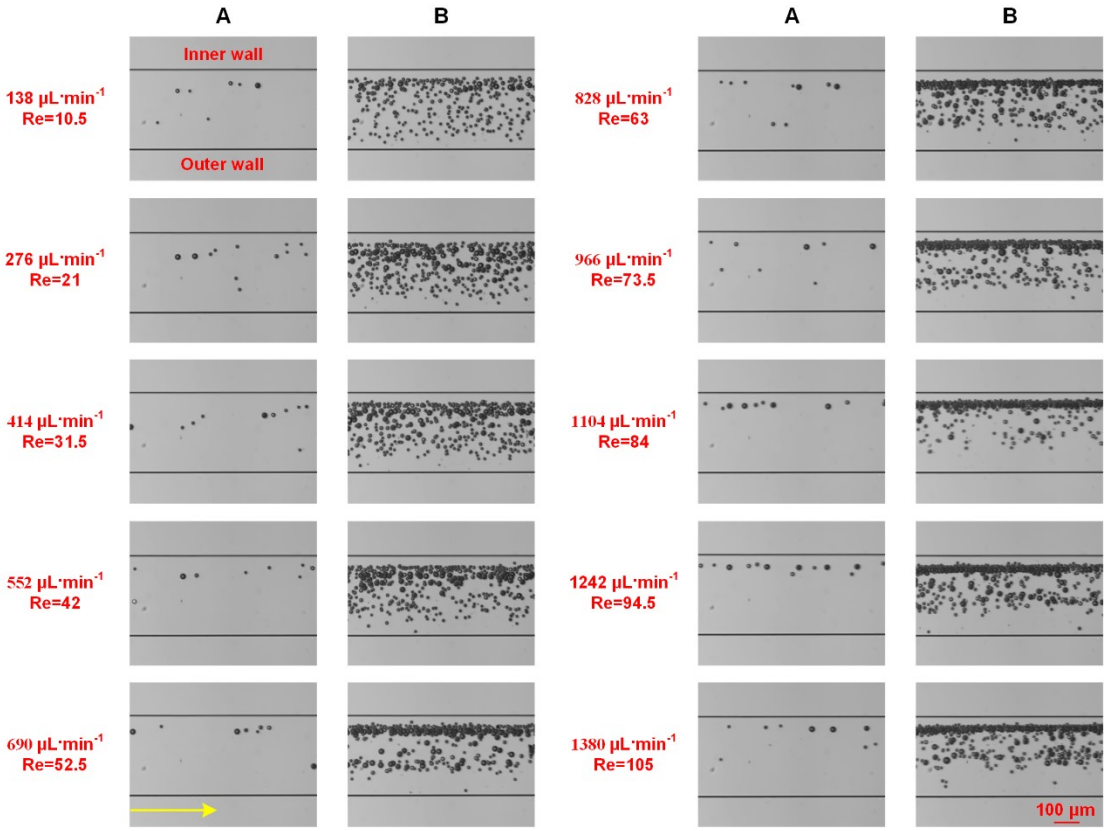

Fig. S10 (A) The images of focused multi-sized particles captured by a high-speed CCD camera at flow rates of 138 μL·min^{-1} to 1,380 μL·min^{-1} (Re: 10.5 ~ 105) in HMC B. A particle mixture with a ratio of 1:1:1:1 of 10 μm, 12 μm, 15 μm, and 20 μm particles are prepared for the co-focusing experiments. The yellow arrow shows the fluid flow direction. (B) The composite images of focused multi-sized particles using 50 single images at flow rates of 138 μL·min^{-1} to 1,380 μL·min^{-1} (Re: 10.5 ~ 105) in HMC B. The scale bar is 100 μm. More images can be provided by reasonable requirements.

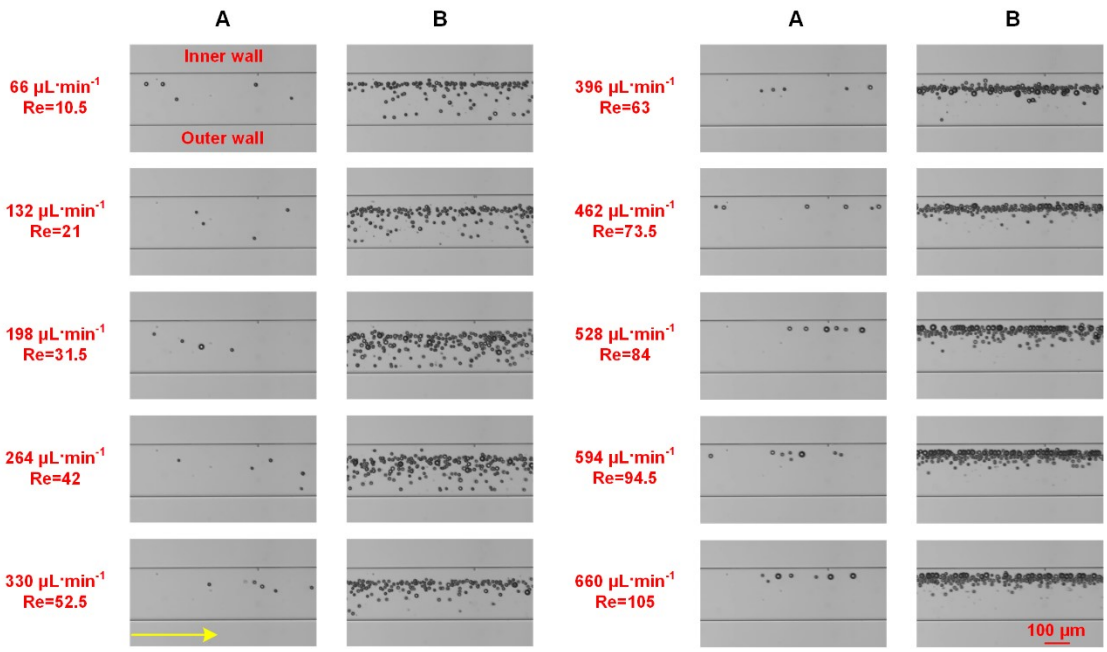

Fig. S11 (A) The images of focused multi-sized particles captured by a high-speed CCD camera at flow rates of 66 μL·min^{-1} to 660 μL·min^{-1} (Re: 10.5 ~ 105) in HMC C. A particle mixture with a ratio of 1:1:1:1 of 10 μm, 12 μm, 15 μm, and 20 μm particles are prepared for the co-focusing experiments. The yellow arrow shows the fluid flow direction. (B) The composite images of focused multi-sized particles using 50 single images at flow rates of 66 μL·min^{-1} to 660 μL·min^{-1} (Re: 10.5 ~ 105) in HMC C. The scale bar is 100 μm. More images can be provided by reasonable requirements.

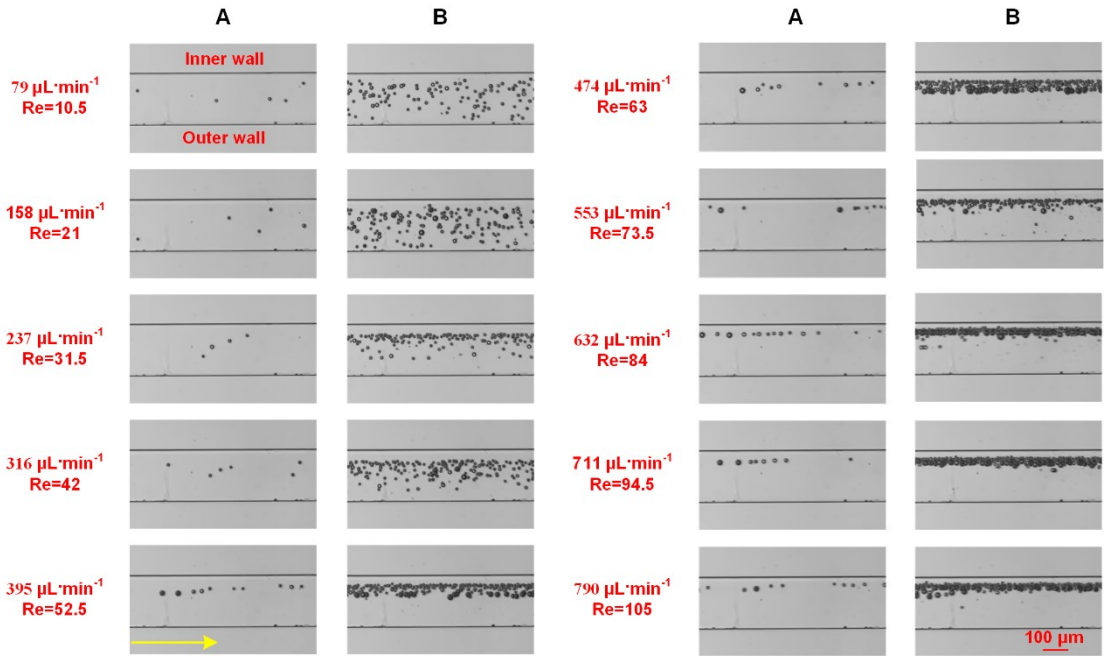

Fig. S12 (A) The images of focused multi-sized particles captured by a high-speed CCD camera at flow rates of 79 μL·min^{-1} to 790 μL·min^{-1} (Re: 10.5 ~ 105) in HMC D. A particle mixture with a ratio of 1:1:1:1 of 10 μm, 12 μm, 15 μm, and 20 μm particles are prepared for the co-focusing experiments. The yellow arrow shows the fluid flow direction. (B) The composite images of focused multi-sized particles using 50 single images at flow rates of 79 μL·min^{-1} to 790 μL·min^{-1} (Re: 10.5 ~ 105) in HMC D. The scale bar is 100 μm. More images can be provided by reasonable requirements.

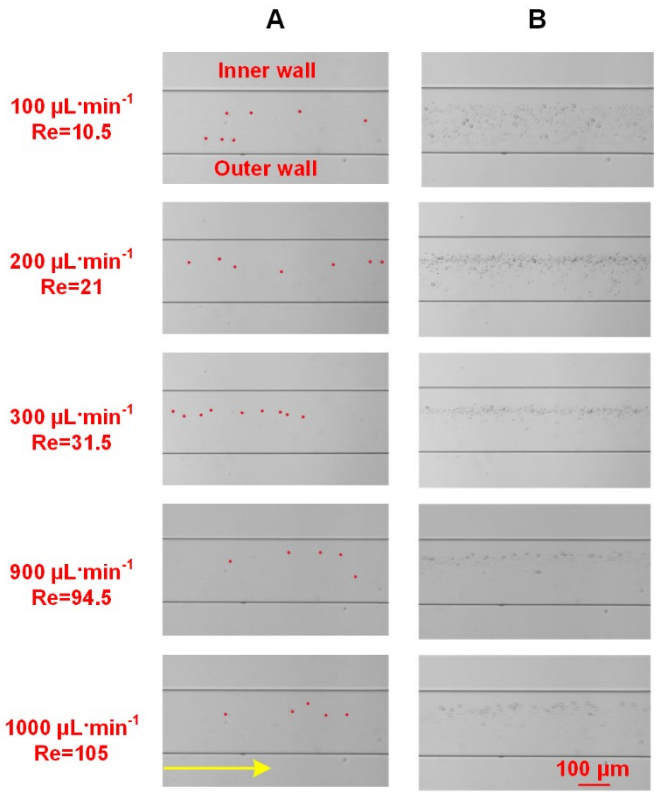

Fig. S13 (A) The images of focused WBCs captured by a high-speed CCD camera at flow rates of 100 μL·min^{-1}, 200 μL·min^{-1}, 300 μL·min^{-1}, 900 μL·min^{-1} and 1,000 μL·min^{-1} in HMC A. The WBCs are indicated using red dots, since they were transparent and can hardly be seen in processed figures. Original images showing WBCs focusing are provided in Supplementary materials. The yellow arrow shows the fluid flow direction. (B) The composite images of focused WBCs using 50 single images at flow rates of 100 μL·min^{-1}, 200 μL·min^{-1}, 300 μL·min^{-1}, 900 μL·min^{-1} and 1,000 μL·min^{-1} in HMC A. The scale bar is 100 μm. More images can be provided by reasonable requirements.